

High-Efficiency in Vitro and in Vivo Detection of Zn²⁺ by Dye-Assembled Upconversion Nanoparticles

Juanjuan Peng,^{†,⊥} Wang Xu,^{‡,⊥} Chai Lean Teoh,[†] Sanyang Han,[‡] Beomsue Kim,[†] Animesh Samanta,[†] Jun Cheng Er,[‡] Lu Wang,[‡] Lin Yuan,[‡] Xiaogang Liu,^{‡,§,||} and Young-Tae Chang^{*,†,‡}

[†]Singapore Bioimaging Consortium, Agency for Science, Technology and Research (A* STAR), 138667, Singapore

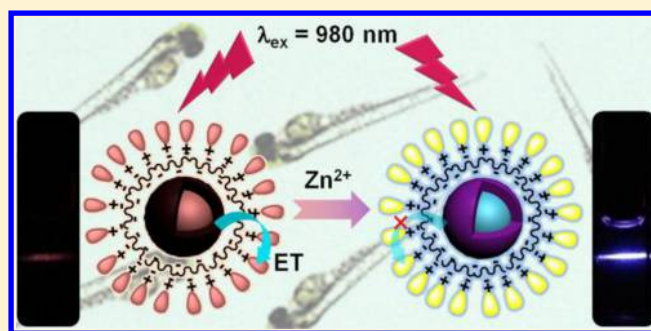
[‡]Department of Chemistry, National University of Singapore, 117543, Singapore

[§]Institute of Materials Research and Engineering, Agency for Science, Technology and Research (A* STAR), 117602, Singapore

^{||}Center for Functional Materials, NUS (Suzhou) Research Institute, Suzhou, Jiangsu 215123, China

Supporting Information

ABSTRACT: Development of highly sensitive and selective sensing systems of divalent zinc ion (Zn²⁺) in organisms has been a growing interest in the past decades owing to its pivotal role in cellular metabolism, apoptosis, and neurotransmission. Herein, we report the rational design and synthesis of a Zn²⁺ fluorescent-based probe by assembling lanthanide-doped upconversion nanoparticles (UCNPs) with chromophores. Specifically, upconversion luminescence (UCL) can be effectively quenched by the chromophores on the surface of nanoparticles via a fluorescence resonant energy transfer (FRET) process and subsequently recovered upon the addition of Zn²⁺, thus allowing for quantitative monitoring of Zn²⁺. Importantly, the sensing system enables detection of Zn²⁺ in real biological samples. We demonstrate that this chromophore–UCNP nanosystem is capable of implementing an efficient in vitro and in vivo detection of Zn²⁺ in mouse brain slice with Alzheimer's disease and zebrafish, respectively.



of Zn²⁺ in real biological samples. We demonstrate that this

INTRODUCTION

As the second most abundant d-block metal ion in human brain and an active component in enzymes and proteins,¹ Zn²⁺ plays an important role in life processes including gene expression and neurotransmission.² The extent of Zn²⁺ deficiency is also associated with physical growth retardation and neurological disorder such as cerebral ischemia and Alzheimer's disease (AD).³ Therefore, there is an increasing demand for highly sensitive analytical methods for the detection of Zn²⁺. The in vivo temporal and spatial detection of Zn²⁺ is challenging but essential to address Zn²⁺-related issues. Tremendous efforts have been devoted to developing sensitive Zn²⁺-monitoring approaches.⁴ Among them, fluorescence spectroscopy is particularly useful owing to its high sensitivity, ease of use, and ability to facilitate real-time detection.⁵ Previously published fluorescent Zn²⁺ probes based on organic dyes and inorganic nanoparticles are summarized in Table S1 in Supporting Information.

Lanthanide-doped upconversion nanoparticles (UCNPs), which are capable of converting near-infrared (NIR) excitation light to short wavelength emissions, have emerged as a promising luminescent probe in potential applications in sensing and bioimaging owing to their intriguing characteristics, such as a large anti-Stokes shift of up to several hundred nanometers, non-autofluorescence from biosamples, high

penetration depth, and no photobleaching.⁶ Alternatively, chromophores with specific recognition sites are widely used for highly selective sensing systems. Therefore, the integration of UCNPs and chromophores endows the hybrid system with the outstanding recognition properties of chromophores and remarkable imaging capacity from UCNPs, thus producing highly sensitive and selective sensing system based on fluorescence resonance energy transfer (FRET) process between them. Till now, a number of UCNPs-based FRET systems have been developed to detect various analytes, such as DNA,⁷ O₂,⁸ CN⁻,⁹ NH₄⁺,¹⁰ and Hg²⁺.¹¹ To the best of our knowledge, UCNPs-based selective fluorescence probes for Zn²⁺ detection in real biological samples have yet been reported.

To address this need, we have developed multilayered UCNPs modified with polyacrylic acid and compound **1**, respectively, as probes (abbreviated as **1**-PAA-UCNPs shown in Figure 1) for sensitive and rapid monitoring of Zn²⁺ ions. A FRET process with NaYF₄:Yb/Tm@NaYF₄ (20/0.2 mol %) as the energy donor and Zn²⁺-responsive compound **1** as the acceptor was constructed. Formation of a Zn–**1** complex inhibits the FRET, thus enabling the detection of Zn²⁺ in

Received: November 17, 2014

Published: January 27, 2015

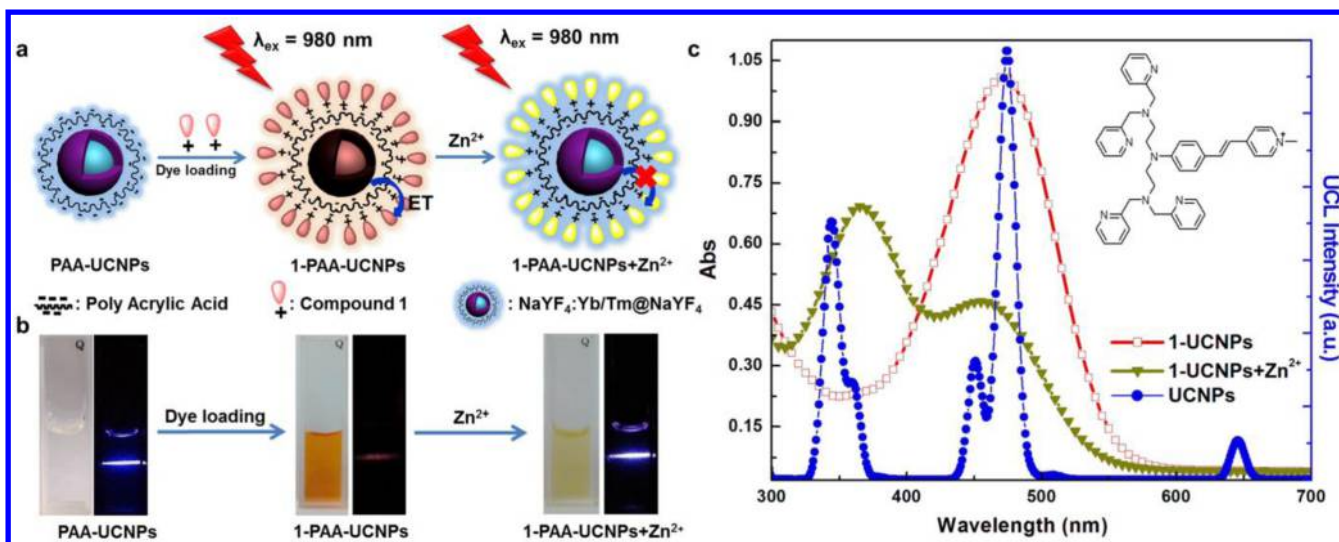


Figure 1. (a) Schematic illustration showing the synthesis of chromophore-assembled UCNP and their response to Zn²⁺. (b) Photographs showing the solution (left) and corresponding upconversion luminescence (right) of PAA-UCNPs (1 mg/mL), 1-PAA-UCNPs (1 mg/mL), and 1-PAA-UCNP with Zn²⁺ (120 μM), respectively. (c) UV-vis spectra of compound 1 measured in the absence (red line, 0.1 mM) and presence (dark yellow line, 120 μM) of Zn²⁺ and UCL spectrum of PAA-UCNPs (blue line). Inserted is the molecular structure of compound 1.

aqueous solution. Importantly, this hybrid nanoprobe is also applicable for upconversion luminescence (UCL) imaging of Zn²⁺-rich amyloid brain tissues with AD. We further demonstrate its capability to detect endogenous Zn²⁺ in a living animal model of zebrafish.

RESULTS AND DISCUSSION

Design Principle of the UCL Nanosensor for Zn²⁺. Our designed sensing system relies on a FRET process in 1-PAA-UCNPs for detection of Zn²⁺ (Figure 1a). In this process, NaYF₄:Yb/Tm@NaYF₄ upconversion nanocrystals with blue UCL were used as energy donor. Alternatively, a Zn²⁺ responsive compound 1 assembled on the surface of upconversion nanocrystals was chosen as energy acceptor because of large overlapping between its absorption band with the UCL. In the absence of Zn²⁺, the UCNP gives rise to blue emissions originating from the ¹G₄ → ³H₆ transition of Tm³⁺ under the excitation of a 980 nm laser. This UCL could be quenched by compound 1 with a strong absorbance band centered at 475 nm (Figure 1c), which is accompanied by the reduction in the I_{475 nm}/I_{654 nm} ratio of UCL. In the presence of Zn²⁺, the coordination of Zn²⁺ with the compound 1 could lead to a significant blue shift of the absorbance of 1-PAA-UCNPs from 475 to 360 nm due to the intramolecular charge transfer of compound 1 (Figure S1), thereby resulting in energy mismatch between the absorption of compound 1 and the blue emission of UCNP. Therefore, the energy transfer (ET) from the UCNP to compound 1 is suppressed, while the UCL signal located at 475 nm can be recovered. This variation in UCL intensity allows us to achieve quantitative monitoring of Zn²⁺. On a separate note, the absorption band of compound 1 shows no overlap with the red emission (¹G₄ → ³F₄ transition) of Tm³⁺ at 654 nm upon the addition of Zn²⁺, which could be used as an inner reference to determine the Zn²⁺ concentration.

Synthesis and Characterization of 1-PAA-UCNPs. In the present study, in order to obtain effective UCL, pure hexagonal-phase core-shell UCNP with an average diameter of ~16 nm (Figure 2a, Figure 2c, Figure S2, and Figure S3) were prepared according to the literature.¹² In a typical

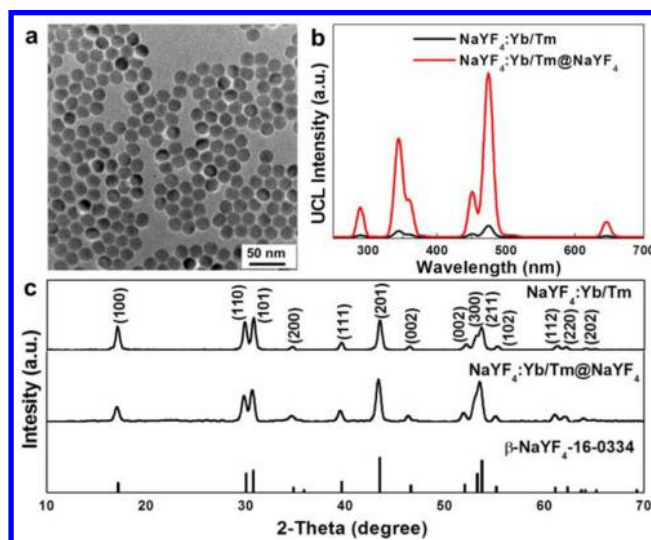


Figure 2. (a) TEM images of NaYF₄:Yb/Tm(20/0.2 mol %)/NaYF₄ core-shell nanocrystals. (b) Upconversion luminescence spectra of the NaYF₄:Yb/Tm (20/0.2% mol %) and NaYF₄:Yb/Tm(20/0.2% mol %)/NaYF₄ UCNP under the 980 nm excitation. (c) X-ray powder diffraction pattern of the as-prepared NaYF₄:Yb/Tm core and NaYF₄:Yb/Tm@NaYF₄ core-shell nanoparticles, showing that all peaks can be well indexed in accordance with pure hexagonal NaYF₄ (JCPDS card no.15-0334).

procedure, NaYF₄:Yb/Tm (20/0.2 mol %) nanocrystals were first synthesized as the core and subsequently coated by NaYF₄ shell through the epitaxial growth. The core-shell design can minimize surface quenching induced energy loss¹³ and improve the UCL emission intensity by 10 times (Figure 2b). To integrate UCNP and compound 1 together into one nanosystem, the oleic acid (OA) ligands on the surface of UCNP were first replaced by negatively charged hydrophilic PAA.¹⁴ It should be noted that the size and morphology of nanocrystals did not change during the ligand exchange process (Figures S4 and S5). Then the positively charged compound 1 was assembled onto the UCNP surface through electrostatic

attraction. With increasing concentrations of compound **1**, the UCL intensity of UCNP remarkably decreased (Figure S6). The absorption spectroscopy result revealed that the amount of compound **1** on the surface of the UCNP was 0.58×10^{-4} M, which was approximately 7.6 wt % of the 1-PAA-UCNPs (Figure S7). To prove the stability of 1-PAA-UCNPs in biological environments, the as-prepared nanoprobe were dispersed in different media, such as water, PBS (0.1 M, pH = 7.0), HEPES (1 M, pH = 7.0), DMEM medium (containing 10% FBS), or cell extracts, and kept for 24 h prior to the measurement of UCL (Figure S8). It was found that the UCL signals remained essentially constant as compared to the nonincubated solution counterparts, clearly suggesting that the developed nanoprobe is feasible for applications in biological settings.

Zn²⁺-Sensing Capabilities of 1-PAA-UCNPs. To examine the effect of Zn²⁺ concentration on the optical properties of 1-PAA-UCNPs, we added different concentrations of Zn²⁺ into the aqueous solution containing as-prepared nanoprobe. As expected, upon addition of Zn²⁺ to the solution of 1-PAA-UCNPs, a significant increase in the UCL intensity at 475 nm could be observed owing to the blue shift absorption of compound **1** (Figure 3a, Figure 3b, and Figure S9). Significantly, we surprisingly found that the variation of color and UCL has fast response within 5 s (Figure S10, movie in Supporting Information).

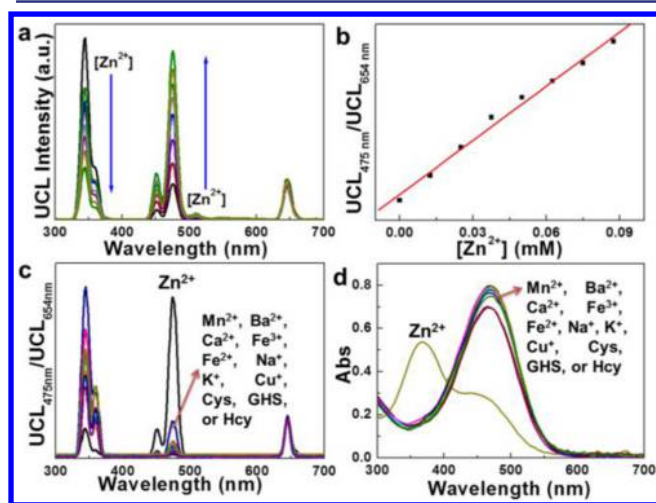


Figure 3. (a) Photoluminescence response of 1-PAA-UCNPs solutions (1 mg/mL) as a function of Zn²⁺ concentration (0–0.09 mM) in an aqueous solution (normalized to 654 nm emission). (b) Plot of luminescence intensity at UCL_{475 nm}/UCL_{654 nm} against the Zn²⁺ concentration. (c) UCL spectra of 1-PAA-UCNPs solutions (1 mg/mL) in the presence of different cations (0.1 mM each), amino acids, and peptide (Cys, Hcy, GHS, 0.2 mM). (d) UV–vis absorption spectra of 1-PAA-UCNPs solutions (1 mg/mL) upon addition of different cations (0.1 mM), amino acids, and GSH (0.2 mM).

To further investigate the selectivity of 1-PAA-UCNPs sensors, we tested a series of solutions including various biological metal ions, amino acid including cysteine (Cys), homocysteine (Hcy), and glutathione (GHS). As shown in Figure 3c, only Zn²⁺ could induce obvious signal change of 1-PAA-UCNPs. In contrast, other metal ions (e.g., Ca²⁺, Fe³⁺, Mn²⁺, Ba²⁺, Na⁺, K⁺) and amino acids did not result in any response of UCL signals. In addition, only the addition of Zn²⁺ led to drastic blue shift of the compound **1** absorption (Figure

3d), further suggesting the good selectivity of our sensor. Therefore, 1-PAA-UCNPs could act as a highly selective UCL probe for Zn²⁺ in vivo without the interference from other metals

Sensing of Zn²⁺ in Living Cells. To demonstrate the potential use of 1-PAA-UCNPs for bioimaging applications, the cytotoxicity of both PAA-UCNPs and 1-PAA-UCNPs was evaluated on the basis of the reduction activity of methylthiazolyltetrazolium (MTT) assay. In our study, two kinds of cell lines (HeLa (cervical carcinoma) and OSCC (oral squamous cell carcinoma)) were selected. The cell viabilities of two cell line are both higher than 95% with the exposure of a dose of 600 μg/mL for 24 h (Figures S11 and S12), suggesting that PAA-UCNPs and 1-PAA-UCNPs have excellent biocompatibility. To investigate the capability of 1-PAA-UCNPs for monitoring Zn²⁺ in cells, the cells were incubated with the nanoparticles (500 μg/mL) for 2 h and analyzed under an optical fluorescence microscope equipped with a 980 nm laser. Blue UCL emitted by PAA-UCNPs without assembling of compound **1** can be clearly observed from the cells, indicating the cellular uptake of the PAA-coated nanoparticles (Figure S13a,b). On the other hand, only dim blue UCL can be observed from the cells treated with 1-PAA-UCNPs (Figure S13c,d), while the blue UCL can be largely recovered by treatment of Zn²⁺ (0.25 mM) for 30 min (Figure S13e,f). By monitoring of the variation of the UCL intensity from the cells in the presence or absence of Zn²⁺, a semiquantitative detection could be achieved (Figures S13 and S14). Taken together, these results confirm the feasibility of intracellular Zn²⁺ monitoring by 1-PAA-UCNPs.

Screening of β-Amyloid in Brain Tissue. AD is characterized by the presence of β-amyloid deposits in the brain, and oxidative stress has been implicated to play a crucial role in the pathogenesis.¹⁵ Many recent studies have implicated metals to be crucial in the development or progression of AD.¹⁶ Among these biometals, zinc is significant because of its ability to catalyze oxidative damage and modulate Alzheimer β-amyloid precursor protein processing.¹⁷ To further validate the capability of our nanoprobe for monitoring Zn²⁺ ions in biological tissue, the triple transgenic knock-in mouse (APPsw/P301L tau/PSEN1M146) brain with AD was chosen as the model in our study owing to the high concentration of Zn²⁺ ions in the β-amyloid plaques.¹⁸ We next incubated AD brain tissue with 1-PAA-UCNPs and analyzed using a fluorescence microscope. As shown in Figure 4a,b, blue UCL spots can be observed from the brain tissue with AD treated by 1-PAA-UCNPs. We further pretreated brain slices with Zn²⁺. After incubation with 1-PAA-UCNPs (Figure 4c,d), we surprisingly found that the pretreatment led to much stronger UCL due to the concentrated Zn²⁺ in β-amyloid. To verify that the UCL recovery originated from Zn²⁺, wild-type brain tissue (W/T) from normal mouse was employed. As shown in Figure 4e,f, very weak UCL could be observed from imaging of the W/T tissue with a small amount of Zn²⁺.¹⁹ In another set of control experiments, EDTA was used to inhibit the coordination between compound **1** and Zn²⁺ owing to its strong chelation property. We pretreated brain tissue with EDTA. As a result, almost no emission from brain tissue with 1-PAA-UCNPs could be detected (Figure 4g,h), indicating good selectivity of our sensor. In addition, the comparison of UCL intensity from tissue images reveals that our probes enable the semiquantitative detection of Zn²⁺ in brain tissue (Figure S15). Taken together,

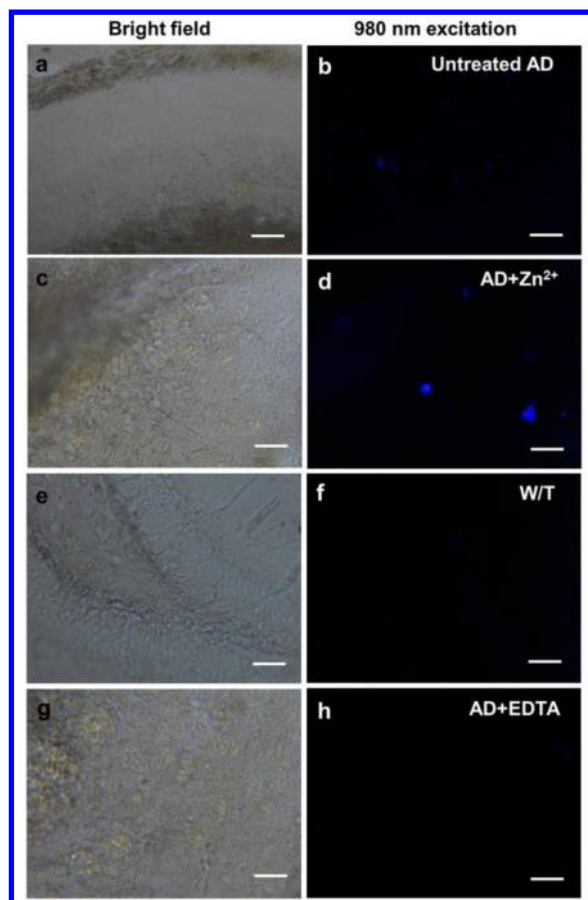


Figure 4. Bright-field and upconversion luminescence images of (a, b) AD brain tissue without treatment, (c, d) AD brain tissue preincubation with $100 \mu\text{M}$ ZnCl_2 for 1 h, (e, f) wild-type tissue (W/T), (g, h) AD brain tissue preincubation with 5 mM EDTA for 2 h, then stained with 1-PAA-UCNPs ($500 \mu\text{g}/\text{mL}$). The scale bars are $10 \mu\text{m}$.

these results suggest that our designed nanoprobe can be promising probes for Zn^{2+} detection in biosamples.

In Vivo Zn^{2+} Detection in Zebrafish. Encouraged by the results of the in vitro cell imaging and brain tissue studies, we further investigated the in vivo detection in living animal. In our experiment, zebrafish was chosen as model. The transparent zebrafish larva is an ideal animal model to monitor analytes using fluorescent sensors because of convenient detection of ions by fluorescence microscopy and permeability of ions and sensors in its body.²⁰ Therefore, zebrafish has been widely used to detect various ions such as Cu^{2+} , Ca^{2+} , and Zn^{2+} .²¹ As a proof of concept experiment, we incubated 1-PAA-UCNPs with the living zebrafish and then traced the biodistribution of intact Zn^{2+} inside zebrafish by fluorescence microscopic imaging. As shown in Figure 5, the bright luminescence of 1-PAA-UCNPs could be clearly observed around its ventricle (parts b, d, f, and h of Figure 5, encircled and arrow pointed). From the zoomed image of a part of the head in Figure 5h, it can be found that the bright luminescent dots were located at its eyes. We attributed it to the high concentration of Zn^{2+} in this position which might be the neuromasts of the anterior lateral-line system (ALL system) of zebrafish larva for the perception of the water flow.^{22,4b} As a control experiment, 3-day-old zebrafish were first exposed to EDTA ($250 \mu\text{M}$ for 2 h) before the treatment of 1-PAA-UCNPs (Figure 5j, Figure 5i). The

imaging result shows that the obtained UCL signals in the fish significantly decreased. Furthermore, by quantitative analysis of UCL signals from the zebrafish before and after treatment with EDTA (Figure S16), it can also be found that the UCL intensity decreased significantly after EDTA treatment. All results suggest that the fluorescence resulted from endogenous Zn^{2+} in zebrafish. Therefore, we can conclude that our 1-PAA-UCNPs-based sensing system offers an exciting platform for in vivo Zn^{2+} detection.

CONCLUSIONS

In summary, we have developed a promising sensing platform using 1-modified upconversion nanoprobe for rapid and sensitive detection of Zn^{2+} in aqueous solution. This detection nanosystem exhibited high sensitivity down to $0.78 \mu\text{M}$ and quick response within 5 s. Taking advantage of the good selectivity of compound 1 and the intriguing optical properties offered by UCNPs, we have also demonstrated our hybrid nanoprobe were also applicable for in vitro and in vivo Zn^{2+} detection in the amyloid plaque in AD brain and zebrafish, respectively. Our sensing system provides a new opportunity for disease diagnosis associated with Zn^{2+} in further clinical medicine.

EXPERIMENTAL SECTION

Materials. $\text{Y}(\text{CH}_3\text{CO}_2)_3 \cdot x\text{H}_2\text{O}$ (99.9%), $\text{Yb}(\text{CH}_3\text{CO}_2)_3 \cdot 4\text{H}_2\text{O}$ (99.9%), $\text{Tm}(\text{CH}_3\text{CO}_2)_3 \cdot x\text{H}_2\text{O}$ (99.9%), NaOH (98+%), NH_4F (98+%), 1-octadecene (90%), oleic acid (OA) (90%), and HCl were purchased from Sigma-Aldrich and used as received without further purification.

Characterization. TEM measurements were carried out on a JEL-1400 transmission electron microscope (JEOL) operating at an acceleration voltage of 100 kV. UCL spectra were obtained with a DM150i monochromator equipped with a R928 photon counting photomultiplier tube (PMT), in conjunction with a 980 nm diode laser. UV-vis spectra were obtained using a fluorimeter and UV/vis instrument, SpectraMax M2, Molecular Devices. Cell imaging was performed on an Olympus BX51 microscope with a xenon lamp adapted to a 980 nm diode laser. The excitation laser power was adjusted to 2.5 W, and luminescence micrographs were recorded with a Nikon DS-R1i color imaging system. Image analysis was performed using NIS-Elements Advanced Research software (Nikon).

Synthesis of $\beta\text{-NaYF}_4\text{:Yb/Tm}$ (20/0.2 mol %) Core Nanoparticles. In a typical experiment, a water solution (2 mL) containing $\text{Y}(\text{CH}_3\text{CO}_2)_3$ (0.32 mmol), $\text{Yb}(\text{CH}_3\text{CO}_2)_3$ (0.08 mmol), and $\text{Tm}(\text{CH}_3\text{CO}_2)_3$ (0.0008 mmol) was added to a 50 mL flask containing oleic acid (3 mL) and 1-octadecene (7 mL). The resulting mixture was heated to $150 \text{ }^\circ\text{C}$ for 1.5 h to form lanthanide oleate complexes and remove water and then cooled to $50 \text{ }^\circ\text{C}$. Subsequently, a methanol solution (6 mL) containing NH_4F (1.6 mmol) and NaOH (1 mmol) was added and stirred at $50 \text{ }^\circ\text{C}$ for 0.5 h. The reaction mixture was heated to $100 \text{ }^\circ\text{C}$ to remove the methanol. Upon removal of the methanol, the solution was heated to $290 \text{ }^\circ\text{C}$ for 1.5 h under an argon flow, at which time the mixture was cooled to room temperature. The resulting nanoparticles were precipitated out by the addition of ethanol, collected by centrifugation, washed with ethanol and cyclohexane, and finally redispersed in cyclohexane.

Synthesis of $\text{NaYF}_4\text{:Yb/Tm@NaYF}_4$ Core-Shell Nanoparticles. The core-shell nanoparticles were synthesized according to reported procedure.²³ To a 50 mL flask containing oleic acid (3 mL) and 1-octadecene (7 mL) was added a solution of $\text{Y}(\text{CH}_3\text{CO}_2)_3$ (0.4 mmol) in water. The mixture was then heated to $150 \text{ }^\circ\text{C}$ for 1.5 h with magnetic stirring and then cooled to $50 \text{ }^\circ\text{C}$. $\text{NaYF}_4\text{:Yb/Tm}$ core nanoparticles in cyclohexane were added along with a 6 mL of methanol solution of NH_4F (1.6 mmol) and NaOH (1 mmol). The resulting mixture was stirred at $50 \text{ }^\circ\text{C}$ for 30 min, at which time the reaction temperature was increased to $100 \text{ }^\circ\text{C}$ to remove the methanol.

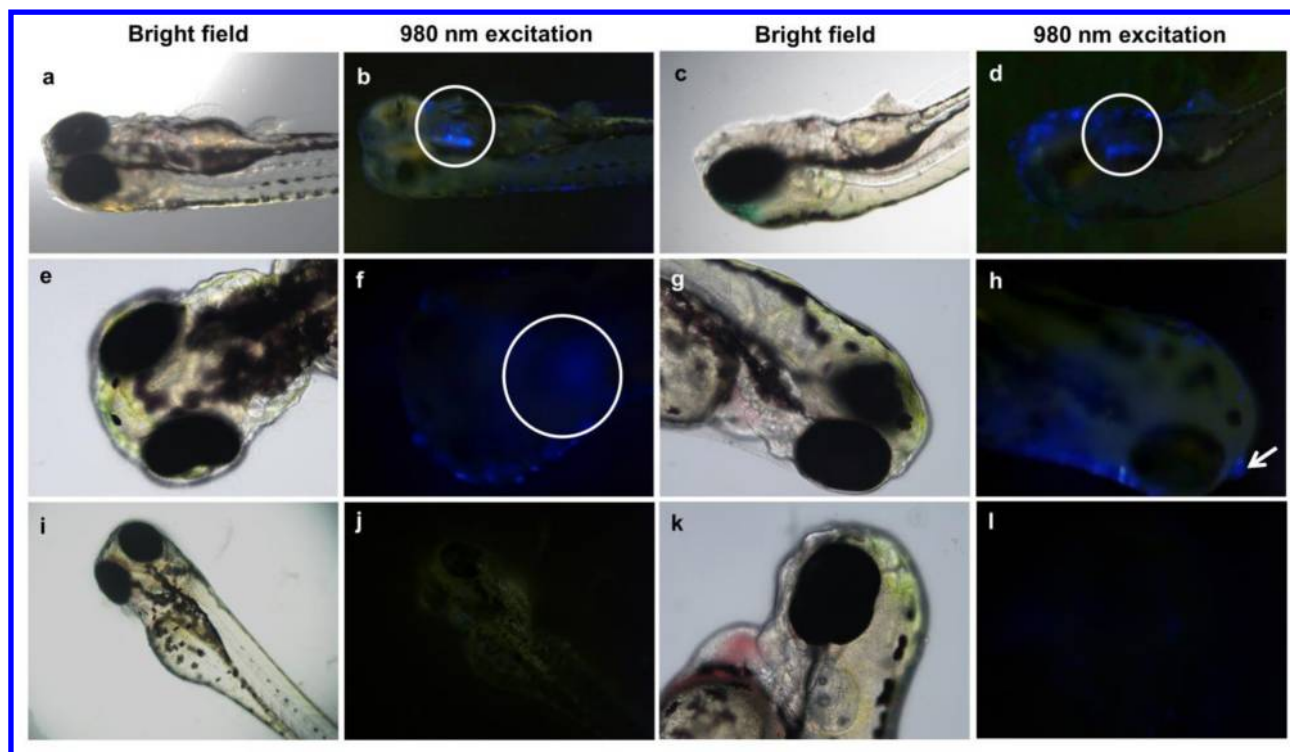


Figure 5. Bright-field (a, c, e, g) and upconversion luminescence images (b, d, f, h) of 3-day-old zebrafish incubated with 500 $\mu\text{g}/\text{mL}$ 1-PAA-UCNPs for 2 h and bright-field (i, k) and upconversion luminescence images (j, l) of zebrafish incubated with EDTA, 250 μM , for 2 h before 1-PAA-UCNPs (500 $\mu\text{g}/\text{mL}$) were incubated for 2 h; the total length is ~ 3 mm.

Then the solution was heated to 290 $^{\circ}\text{C}$ under an argon flow for 1 h and cooled to room temperature. The resulting nanoparticles were precipitated out by the addition of ethanol, collected by centrifugation, washed with ethanol and cyclohexane, and redispersed in cyclohexane.

Preparation of Hydrophilic $\text{NaYF}_4\text{:Yb/Tm@NaYF}_4$ Core-Shell Nanoparticles. The preparation of the ligand free $\text{NaYF}_4\text{:Yb/Tm@NaYF}_4$ was performed as previously reported.^{14a} First, the OA ligands on the surface of $\text{NaYF}_4\text{:Yb/Tm@NaYF}_4$ were washed with hydrochloric acid, and water-dispersible, ligand-free $\text{NaYF}_4\text{:Yb/Tm@NaYF}_4$ was obtained. Then ligand-free UCNPs were dispersed in 10 mg/mL PAA solution (adjusted to pH 7 with NaOH), followed by stirring for 12 h, and PAA-UCNPs were obtained. Finally, the PAA-UCNPs were washed with distilled water by sonication and centrifugation.

Assembling Compound 1 to PAA-UCNPs. 10 mM compound 1 in CH_2Cl_2 (0.2 mL) solution was added dropwise into a water solution containing PAA-UCNPs (1 mg/mL). The solution was then stirred overnight. Free compound 1 was removed by centrifugation. The precipitate was washed with water by centrifugation. The as-obtained hybrid materials (1-PAA-UCNPs) were redispersed by a brief sonication to form a homogeneous solution and stored at 4 $^{\circ}\text{C}$.

Procedures for Ions Sensing. Stock solutions of the ions (2.5 mM) were prepared in H_2O . A stock solution of 1-PAA-UCNPs (1 mg/mL) was prepared in water solution. The sensing of 1-PAA-UCNPs to Zn^{2+} was performed by adding different amount of Zn^{2+} stock solution to 100 μL solution of 1-PAA-UCNPs, respectively. Test samples for selectivity experiments were prepared by adding appropriate amounts of ions stock solution with a similar procedure, and fluorescent spectra of the samples were recorded.

Movie. Real-time color change of 1-PAA-UCNPs aqueous solution upon addition of Zn^{2+} aqueous solution (3 μL , 100 mM) can be observed in the movie file in Supporting Information, and the color was changed from orange to yellow within 5 s.

Cell Culture. The cell lines HeLa and OSCC cells were grown in DMEM medium supplemented with 10% (v/v) fetal bovine serum (FBS) and antibiotics (100 U/mL antibiotic/100 mg/mL antimycotic) in a humidified atmosphere at 37 $^{\circ}\text{C}$ with 5% (v/v) CO_2 .

Cytotoxicity of 1-PAA-UCNPs. To study the cytotoxicity, we dispensed 100 μL of cell suspension (~ 5000 cells/well) in a 96-well plate. The cells were preincubated for 24 h in high glucose media (DMEM) with 10% fetal bovine serum (FBS) and 1% Anti-Anti with in a humidified incubator (37 $^{\circ}\text{C}$, 5% CO_2). Next, different concentrations of PAA-UCNPs, 1-PAA-UCNPs (0, 100, 200, 300, 400, 500, and 600 $\mu\text{g}/\text{mL}$, diluted in DMEM) were then added to the wells. The cells were subsequently incubated for 12 or 24 h at 37 $^{\circ}\text{C}$ under 5% CO_2 . Then MTT (20 μL , 5 mg/mL) was added to each well, and the plate was incubated for an additional 4 h at 37 $^{\circ}\text{C}$ under 5% CO_2 . After the addition of 100 μL of DMSO, the assay plate was allowed to stand at room temperature for 2 h. The optical density OD_{570} value (Abs) of each well, with background subtraction at 690 nm, was measured by means of a fluorimeter and UV/vis instrument, SpectraMax M2, Molecular Devices. The following formula was used to calculate the inhibition of cell growth:

$$\text{cell viability (\%)} = \frac{\text{mean Abs value of treatment group}}{\text{mean Abs value of control}} \times 100$$

Cell Imaging. HeLa and OSCC cell lines were maintained at 37 $^{\circ}\text{C}$ in 5% CO_2 in DMEM media, respectively, both supplemented with 10% fetal bovine serum, 100 U/mL penicillin, and 100 mg/mL streptomycin. The cells were plated at around 60–70% confluency 24 h before imaging experiments in 35 mm culture dishes. Prior to imaging experiments, the cells were incubated with UCNPs (500 $\mu\text{g}/\text{mL}$), 1-PAA-UCNPs (500 $\mu\text{g}/\text{mL}$) for 2 h, and the 1-PAA-UCNPs treated cells were incubated with Zn^{2+} (0.25 mM) solution for 30 min. Both cell lines were washed with cell culture media and subsequently imaged at ambient temperature.

Biological Sample Preparation. The 15- to 20-month-old triple transgenic mice (APPsw/P301L tau/PSEN1M146) were sacrificed for tissue harvesting. The mice were perfused with 4% (w/v) paraformaldehyde (PFA), or the brain tissue was rapidly frozen and stored at -80 $^{\circ}\text{C}$ immediately after extraction. Free-floating sections were prepared from the PFA-perfused brain using vibratome (Leica), and 40 μm slices were stored in antifreeze solution at -20 $^{\circ}\text{C}$ until required. Separately, 10 μm sections of rapidly frozen brain were

prepared using a cryostat and picked up on coated slides and stored in a $-20\text{ }^{\circ}\text{C}$ freezer.

Brain Tissue UCL in Vivo Imaging. Sections were mounted on slides and then treated with $500\text{ }\mu\text{g/mL}$ 1-PAA-UCNPs at room temperature. Separately, sections were pretreated with 5 mM EDTA or $100\text{ }\mu\text{M}$ Zn^{2+} solutions for 1 h before staining with 1-PAA-UCNPs. Imaging was done with Nikon DS-R1 color imaging system.

Tracing Distribution of Zn^{2+} in Zebrafish. Zebrafish were kept at $28\text{ }^{\circ}\text{C}$ and maintained at optimal breeding conditions. For mating, male and female zebrafish were maintained in one tank at $28\text{ }^{\circ}\text{C}$ on a 12 h light/12 h dark cycle, and then the spawning of eggs was triggered by giving light stimulation. Zebrafish were maintained in E3 embryo media. Zebrafish at 3 days were incubated with $500\text{ }\mu\text{g/mL}$ 1-PAA-UCNPs for 2 h at $28\text{ }^{\circ}\text{C}$. Alternatively, 3-day zebrafish were exposed to $250\text{ }\mu\text{M}$ EDTA for 2 h at $28\text{ }^{\circ}\text{C}$ to remove intact Zn^{2+} in zebrafish first, and then zebrafish were further incubated with 1-PAA-UCNPs for 2 h at $28\text{ }^{\circ}\text{C}$. The treated zebrafish were imaged by an Olympus BX51 microscope with a xenon lamp adapted to a 980 nm diode laser.

■ ASSOCIATED CONTENT

Supporting Information

Synthesis details of compound **1**, reaction mechanism between compound **1** and Zn^{2+} , Table S1, Figures S1–S16, and a video of reaction upon addition of Zn^{2+} . This material is available free of charge via the Internet at <http://pubs.acs.org>.

■ AUTHOR INFORMATION

Corresponding Author

*chmcyt@nus.edu.sg

Author Contributions

[†]J.P. and W.X. contributed equally.

Notes

The authors declare no competing financial interest.

■ ACKNOWLEDGMENTS

The authors gratefully acknowledge the A*STAR Joint Council Office (JCO), Singapore (Grant 1231AFG028) for financial support.

■ REFERENCES

- (1) Nolan, E. M.; Lippard, S. J. *Acc. Chem. Res.* **2009**, *42*, 193.
- (2) (a) Burdette, S. C.; Lippard, S. J. *Proc. Natl. Acad. Sci. U.S.A.* **2003**, *100*, 3605. (b) Walkup, G. K.; Burdette, S. C.; Lippard, S. J.; Tsien, R. Y. *J. Am. Chem. Soc.* **2000**, *122*, 5644. (c) Kimura, E.; Aoki, S.; Kikuta, E.; Koike, T. *Proc. Natl. Acad. Sci. U.S.A.* **2003**, *100*, 3731.
- (3) Atwood, C. S.; Moir, R. D.; Huang, X.; Scarpa, R. C.; Bacarra, N. M. E.; Romano, D. M.; Hartshorn, M. A.; Tanzi, R. E.; Bush, A. I. *J. Biol. Chem.* **1998**, *273*, 12817.
- (4) (a) Xu, Z.; Baek, K.-H.; Kim, H. N.; Cui, J.; Qian, X.; Spring, D. R.; Shin, I.; Yoon, J. *J. Am. Chem. Soc.* **2009**, *132*, 601. (b) Qian, F.; Zhang, C. L.; Zhang, Y. M.; He, W. J.; Gao, X.; Hu, P.; Guo, Z. *J. Am. Chem. Soc.* **2009**, *131*, 1460. (c) Datta, B. K.; Mukherjee, S.; Kar, C.; Ramesh, A.; Das, G. *Anal. Chem.* **2013**, *85*, 8369. (d) Wang, H.; Sun, C. L.; Yue, Y. H.; Yin, F. F.; Jiang, J. Q.; Wu, H. R.; Zhang, H. L. *Analyst* **2013**, *138*, 5576.
- (5) (a) Wong, B. A.; Friedle, S.; Lippard, S. J. *J. Am. Chem. Soc.* **2009**, *131*, 7142. (b) Xu, Z.; Yoon, J.; Spring, D. R. *Chem. Soc. Rev.* **2010**, *39*, 1996. (c) Burdette, S. C.; Walkup, G. K.; Spingler, B.; Tsien, R. Y.; Lippard, S. J. *J. Am. Chem. Soc.* **2001**, *123*, 7831. (d) Guo, Z.; Kim, G.-H.; Shin, I.; Yoon, J. *Biomaterials* **2012**, *33*, 7818. (e) Meng, X. M.; Wang, S. X.; Li, Y. M.; Zhu, M. Z.; Guo, Q. X. *Chem. Commun.* **2012**, *48*, 4196. (f) Satapathy, R.; Wu, Y. H.; Lin, H. C. *Org. Lett.* **2012**, *14*, 2564.
- (6) (a) Wang, Z. L.; Hao, J. H.; Chan, H. L. W. *J. Mater. Chem.* **2010**, *20*, 3178. (b) Chatterjee, D. K.; Yong, Z. *Nanomedicine (London, U.K.)* **2008**, *3*, 73. (c) Shen, J.; Sun, L. D.; Yan, C. H. *Dalton Trans.* **2008**, 5687. (d) Zhang, F.; Shi, Y. F.; Sun, X. H.; Zhao, D. Y.; Stucky, G. D. *Chem. Mater.* **2009**, *21*, 5237. (e) Chen, G.; Ohulchanskyy, T. Y.; Liu, S.; Law, W.-C.; Wu, F.; Swihart, M. T.; Ågren, H.; Prasad, P. N. *ACS Nano* **2012**, *6*, 2969. (f) Hou, Z. Y.; Li, C. X.; Ma, P. A.; Cheng, Z. Y.; Li, X. J.; Zhang, X.; Dai, Y. L.; Yang, D. M.; Lian, H. Z.; Lin, J. *Adv. Funct. Mater.* **2012**, *22*, 2713. (g) Wang, G. F.; Peng, Q.; Li, Y. D. *Acc. Chem. Res.* **2011**, *44*, 322. (h) He, M.; Huang, P.; Zhang, C. L.; Chen, F.; Wang, C.; Ma, J. B.; He, R.; Cui, D. X. *Chem. Commun.* **2011**, *47*, 9510. (i) Ju, Q.; Tu, D. T.; Liu, Y. S.; Li, R. F.; Zhu, H. M.; Chen, J. C.; Chen, Z.; Huang, M. D.; Chen, X. Y. *J. Am. Chem. Soc.* **2011**, *134*, 1323. (j) Wang, F.; Liu, X. G. *Chem. Soc. Rev.* **2009**, *38*, 976. (k) Zhou, J.; Liu, Z.; Li, F. Y. *Chem. Soc. Rev.* **2012**, *41*, 1323. (l) Zhang, F.; Haushalter, R. C.; Haushalter, R. W.; Shi, Y. F.; Zhang, Y. C.; Ding, K. L.; Zhao, D. Y.; Stucky, G. D. *Small* **2011**, *7*, 1972–1976. (m) Auzel, F. *Chem. Rev.* **2004**, *104*, 139. (n) Lehmann, O.; Kompe, K.; Haase, M. *J. Am. Chem. Soc.* **2004**, *126*, 14935. (o) Park, Y. I.; Kim, H. M.; Kim, J. H.; Moon, K. C.; Yoo, B.; Lee, K. T.; Lee, N.; Choi, Y.; Park, W.; Ling, D.; Na, K.; Moon, W. K.; Choi, S. H.; Park, H. S.; Yoon, S.-Y.; Suh, Y. D.; Lee, S. H.; Hyeon, T. *Adv. Mater.* **2012**, *24*, 5755. (p) Zhang, F.; Braun, G. B.; Shi, Y. F.; Zhang, Y. C.; Sun, X. H.; Reich, N. O.; Zhao, D. Y.; Stucky, G. *J. Am. Chem. Soc.* **2010**, *132*, 2850. (q) Sivakumar, S.; Boyer, J. C.; Bovero, E.; van Veggel, F. C. J. M. *J. Mater. Chem.* **2009**, *19*, 2392. (r) He, G. S.; Tan, L. S.; Zheng, Q.; Prasad, P. N. *Chem. Rev.* **2008**, *108*, 1245. (s) Dong, C. H.; van Veggel, F. C. J. M. *ACS Nano* **2009**, *3*, 123. (t) Liu, J.; Liu, Y.; Bu, W.; Bu, J.; Sun, Y.; Du, J.; Shi, J. *J. Am. Chem. Soc.* **2014**, *136*, 9701. (u) Wang, J.; Deng, R. R.; MacDonald, M. A.; Chen, B. L.; Yuan, J. K.; Wang, F.; Chi, D. Z.; Andy Hor, T. S.; Zhang, P.; Liu, G. K.; Han, Y.; Liu, X. G. *Nat. Mater.* **2014**, *13*, 157. (v) Xie, X. J.; Gao, N. Y.; Deng, R. R.; Sun, Q.; Xu, Q. H.; Liu, X. G. *J. Am. Chem. Soc.* **2013**, *135*, 12608. (w) Shen, J.; Chen, G. Y.; Vu, A.-M.; Fan, W.; Bilsel, O. S.; Chang, C.-C.; Han, G. *Adv. Opt. Mater.* **2013**, *1*, 644. (x) Min, Y. Z.; Li, J. M.; Liu, F.; Yeow, E. K. L.; Xing, B. G. *Angew. Chem.* **2014**, *126*, 1030. (y) Tian, G.; Gu, Z. J.; Zhou, L. J.; Yin, W. Y.; Liu, X. X.; Yan, L.; Jin, S.; Ren, W. L.; Xing, G. M.; Li, S. J.; Zhao, Y. L. *Adv. Mater.* **2012**, *24*, 1226. (z) Lai, J. P.; Zhang, Y. X.; Pasquale, N.; Lee, K.-B. *Angew. Chem., Int. Ed.* **2014**, *53*, 14419.
- (7) (a) Zhang, P.; Rogelj, S.; Nguyen, K.; Wheeler, D. *J. Am. Chem. Soc.* **2006**, *128*, 12410. (b) Kumar, M.; Zhang, P. *Langmuir* **2009**, *25*, 6024.
- (8) Achatz, D. E.; Meier, R. J.; Fischer, L. H.; Wolfbeis, O. S. *Angew. Chem., Int. Ed.* **2010**, *50*, 260.
- (9) (a) Yao, L. M.; Zhou, J.; Liu, J. L.; Feng, W.; Li, F. Y. *Adv. Funct. Mater.* **2012**, *22*, 2667. (b) Liu, J. L.; Liu, Y.; Liu, Q.; Li, C. Y.; Sun, L. N.; Li, F. Y. *J. Am. Chem. Soc.* **2011**, *133*, 15276. (c) Zhao, L. Z.; Peng, J. J.; Chen, M.; Liu, Y.; Yao, L. M.; Feng, W.; Li, F. Y. *ACS Appl. Mater. Interfaces* **2014**, *6*, 11190.
- (10) Mader, H. S.; Wolfbeis, O. S. *Anal. Chem.* **2010**, *82*, 5002.
- (11) (a) Liu, Q.; Peng, J. J.; Sun, L. N.; Li, F. Y. *ACS Nano* **2011**, *5*, 8040. (b) Liu, Y.; Chen, M.; Cao, T. Y.; Sun, Y.; Li, C. Y.; Liu, Q.; Yang, T. S.; Yao, L. M.; Feng, W.; Li, F. Y. *J. Am. Chem. Soc.* **2013**, *135*, 9869.
- (12) Wang, F.; Deng, R. R.; Wang, J.; Wang, Q. X.; Han, Y.; Zhu, H. M.; Chen, X. Y.; Liu, X. G. *Nat. Mater.* **2011**, *10*, 968.
- (13) (a) Boyer, J. C.; Manseau, M. P.; Murray, J. I.; van Veggel, F. C. J. M. *Langmuir* **2010**, *26*, 1157. (b) Zhao, L. Z.; Peng, J. J.; Huang, Q.; Li, C. Y.; Chen, M.; Sun, Y.; Lin, Q. N.; Zhu, L. Y.; Li, F. Y. *Adv. Funct. Mater.* **2013**, *24*, 363.
- (14) (a) Bogdan, N.; Vetrone, F.; Ozin, G. A.; Capobianco, J. A. *Nano Lett.* **2011**, *11*, 835. (b) Cheng, L.; Yang, K.; Chen, Q.; Liu, Z. *ACS Nano* **2012**, *6*, 5605.
- (15) Cirrito, J. Extracellular Amyloid- β Protein Dynamics in Alzheimer's Disease. In *Microdialysis in Drug Development*; Müller, M., Ed.; Springer: New York, 2013; Chapter 9, pp 163–178.
- (16) (a) Adlard, P. A.; Bush, A. I. *J. Alzheimer's Dis.* **2006**, *10*, 145. (b) Crichton, R. R.; Dexter, D. T.; Ward, R. J. *Coord. Chem. Rev.* **2008**, *252*, 1189. (c) Barnham, K. J.; Bush, A. I. *Curr. Opin. Chem. Biol.* **2008**, *12*, 222.

- (17) Bush, A. I.; Pettingell, W. H.; de Paradis, M.; Tanzi, R. E.; Wasco, W. *J. Biol. Chem.* **1994**, *269*, 26618.
- (18) Reshmi, R.; Ren, M.; Maria, D. Y.; Gemma, C.; Mark, A. S.; George, P.; Barry, H.; Frank, W. *Biochem. Biophys. Res. Commun.* **2009**, *382*, 91.
- (19) Emily, L. Q.; Dylan, W. D.; Christopher, J. C. *Chem. Rev.* **2008**, *108*, 1517.
- (20) Hutchinson, R. W.; Cox, A. G.; McLeod, C. W.; Marshall, P. S.; Harper, A.; Dawson, E. L.; Howlett, D. R. *Anal. Biochem.* **2005**, *346*, 225.
- (21) Brustein, E.; Marandi, N.; Kovalchuk, Y.; Drapeau, P.; Konnerth, A. *Pfluegers Arch.* **2003**, *446*, 766.
- (22) Grant, K. A.; Raible, D. W.; Piotrowski, T. *Neuron* **2005**, *45*, 69.
- (23) Wang, F.; Wang, J.; Liu, X. G. *Angew. Chem., Int. Ed.* **2010**, *49*, 7456.